Human Molecular Genetics, 2018, Vol. 27, No. 12 2052–2063

doi: 10.1093/hmg/ddy108
Advance Access Publication Date: 30 March 2018
Original Article

ORIGINAL ARTICLE

The antidepressant tianeptine reverts synaptic AMPA receptor defects caused by deficiency of CDKL5

Marco Tramarin[1,†], Laura Rusconi[1,†], Lara Pizzamiglio[2], Isabella Barbiero[1], Diana Peroni[1], Linda Scaramuzza[3], Tim Guilliams[4], David Cavalla[4,5], Flavia Antonucci[2] and Charlotte Kilstrup-Nielsen[1,*]

[1]Department of Biotechnology and Life Sciences and Center of Neuroscience, University of Insubria, 21052 Busto Arsizio, Italy, [2]Department of Biotechnology and Translational Medicine, University of Milan, 20129 Milan, Italy, [3]San Raffaele Rett Research Unit, Division of Neuroscience, San Raffaele Hospital, 20132 Milan, Italy, [4]Healx Ltd, Park House, Castle Park, Cambridge CB3 0DU, UK and [5]Numedicus Ltd, Cambridge CB1 2DX, UK

*To whom correspondence should be addressed at: Department of Biotechnology and Life Sciences, University of Insubria, Via Manara 7, 21052 Busto Arsizio, Italy. Tel: +39 0331339430; Fax +39 0331339459; Email: c.kilstrup-nielsen@uninsubria.it

Abstract

Mutations in the X-linked cyclin-dependent kinase-like 5 (*CDKL5*) gene cause a complex neurological disorder, characterized by infantile seizures, impairment of cognitive and motor skills and autistic features. Loss of Cdkl5 in mice affects dendritic spine maturation and dynamics but the underlying molecular mechanisms are still far from fully understood. Here we show that Cdkl5 deficiency in primary hippocampal neurons leads to deranged expression of the alpha-amino-3-hydroxy-5-methyl-4-iso-xazole propionic acid receptors (AMPA-R). In particular, a dramatic reduction of expression of the GluA2 subunit occurs concomitantly with its hyper-phosphorylation on Serine 880 and increased ubiquitination. Consequently, Cdkl5 silencing skews the composition of membrane-inserted AMPA-Rs towards the GluA2-lacking calcium-permeable form. Such derangement is likely to contribute, at least in part, to the altered synaptic functions and cognitive impairment linked to loss of Cdkl5. Importantly, we find that tianeptine, a cognitive enhancer and antidepressant drug, known to recruit and stabilise AMPA-Rs at the synaptic sites, can normalise the expression of membrane inserted AMPA-Rs as well as the number of PSD-95 clusters, suggesting its therapeutic potential for patients with mutations in CDKL5.

Introduction

Mutations in the X-linked serine/threonine kinase cyclin-dependent kinase-5 (*CDKL5*) gene are known since 2003 to cause severe neurodevelopmental disorders, referred to as CDKL5 deficiency disorder (CDD). Patients with CDD are characterized by the onset of intractable seizures in the first months after birth, which are accompanied by intellectual disabilities, autistic features, strong hypotonia, sleep disturbances, and gross motor dysfunctions (1,2).

Mouse models with the complete loss of Cdkl5 have been generated and their face validity for CDD is widely recognized (3). Indeed, *Cdkl5*-KO mice mirror various symptoms of the human pathology such as cognitive deficits, impaired motor control, and autistic-like features (4–6). However, differently

[†]The authors wish it to be known that, in their opinion, the first two authors should be regarded as joint First Authors.
Received: February 21, 2018. **Revised:** March 20, 2018. **Accepted:** March 20, 2018

from humans, no spontaneous seizures have been reported in *Cdkl5*-KO mice even if an increased seizure susceptibility to NMDA was recently described (7).

The molecular basis of the abovementioned symptoms linked to loss of CDKL5 is still far from fully understood. However, growing pieces of evidence obtained with *Cdkl5*-KO mice and primary neurons silenced for Cdkl5 expression have accumulated in the last years suggesting a direct role of CDKL5 in controlling synaptic plasticity. The protein is highly abundant in brain where its timing of expression correlates with neuronal maturation (8). Moreover, in neurons CDKL5 dynamically translocates from the nucleus to the cytoplasm where its specific localization and levels are finely tuned by neuronal activity (9,10). CDKL5 is readily detectable in dendritic spines where its synaptic accumulation appears to be regulated both by the dendritic targeting of its mRNA, which undergoes local activity-dependent translation, and through its interaction with post-synaptic density protein 95 (PSD-95) (10–12). In accordance with these data suggesting the involvement of CDKL5 in molecular pathways that regulate synaptic maturation and functioning, Cdkl5 deficiency affects dendritic spine morphology and excitatory functions *in vivo* and *in vitro*. As a matter of fact, neurons devoid of Cdkl5 are characterized by filopodia-like immature dendritic spines, reduced excitatory synaptic puncta, decreased amplitude and frequency of miniature excitatory post-synaptic currents (mEPSCs), and impaired long-term potentiation (LTP) (11–13). Such defects are likely to underlie the cognitive impairment and autistic-like features that are caused by CDKL5 dysfunctions but the rational design of therapeutic strategies for patients with CDD still necessitates a further comprehension of the molecular network belonging to CDKL5 in dendritic spines.

In the current study we show that Cdkl5 deficiency leads to deranged AMPA-R expression. AMPA-Rs mediate most fast excitatory synaptic transmission of the nervous system and are one of the key determinants of synaptic strength and plasticity (14). These glutamatergic receptors are homo- or hetero-tetrameric assemblies made up of combinations of the four subunits GluA1-GluA4. In the adult hippocampus and cortex GluA1-GluA2 hetero-dimers are the predominantly expressed ones. The precise number and subunit composition of AMPA-Rs determines the efficacy and dynamics of AMPA-R mediated synaptic signalling. The number of synaptic AMPA-Rs is extensively regulated through trafficking and degradation under basal conditions and in response to neuronal activity depending on subunit specific post-translational modifications and interacting proteins. The fine-tuning of AMPA-R synaptic expression, trafficking and activity is necessary for proper brain function and many neurological disorders can be linked to synaptic dysfunctions caused by AMPA-R deregulation. For example, AMPA-R subunit variants and altered expression have been associated with mental retardation and dementia (15,16). It is worthwhile mentioning that altered AMPA-R mediated neurotransmission has been linked to autism spectrum disorders (17–19).

Here we show several pieces of evidence linking Cdkl5-associated synaptic defects to aberrant AMPA-R expression. In particular, we find that silencing of Cdkl5 expression in hippocampal neurons has a particularly strong impact on GluA2 levels leaving those of GluA1 less affected. This leads to an apparent imbalance in AMPA-R subunit composition, which we hypothesise may underlie some of the synaptic defects in Cdkl5-deficient neurons. Interestingly, we found that tianeptine, a cognitive enhancer and antidepressant drug known to stabilise AMPA-Rs at the synaptic sites (20), rescued the expression of surface-bound AMPA-Rs and PSD-95, suggesting its therapeutic potential for patients with mutations in CDKL5.

Results

Cdkl5 deficiency specifically influences the expression of the GluA2 AMPA-R subunit

To get further insight into the molecular causes of the cognitive impairment and synaptic defects characterizing CDD, we decided to analyse whether CDKL5 might play a role in regulating AMPA-R expression. To this aim, we silenced primary hippocampal neurons prepared from E17 mouse embryos for Cdkl5 expression with lentiviral particles expressing either of three shRNAs against Cdkl5 or, as control, LacZ (Fig. 1A and B; Supplementary Material, Fig. S1). Total protein levels of GluA1 and GluA2, which are the predominant AMPA-R subunits in hippocampal neurons, were analysed through western blotting (WB) after 16–18 days *in vitro* (DIV) when neurons under our culture conditions have reached the mature state (10). Interestingly, while GluA1 expression was unaltered ($P > 0.05$), Cdkl5 knock-down significantly reduced GluA2 levels (sh#1 0.46 ± 0.10, $P = 0.0003$; sh#2 0.47 ± 0.10, $P = 0.0004$).

This result was further confirmed through immunofluorescence of silenced neurons stained with antibodies against either GluA1 or GluA2, together with GFP and MAP2, allowing to distinguish infected neurons and dendritic branches, respectively (Fig. 1C and D). Indeed, GluA2 staining was significantly reduced (sh#1 0.78 ± 0.04, $P = 0.0125$; sh#2 0.70 ± 0.07, $P = 0.0021$) whereas that of GluA1 was not significantly altered ($P > 0.05$).

To understand whether the observed GluA2 down-regulation is caused by a transcriptional alteration we analysed *GluA2* mRNA levels in silenced neurons through RT-qPCR analysis. As shown in Figure 1E, we did not observe any significant change in *GluA2* transcript levels ($P > 0.05$) indicating that the observed reduction in GluA2 protein expression relies on a post-transcriptional mechanism.

In line with the fundamental role of GluA2 AMPA-R subunits in controlling synaptic activity, its dynamics and turnover are finely regulated in neurons (14). This AMPA-R subunit undergoes constitutive endosomal trafficking, a process that is influenced by its post-translational modifications and through its association with protein partners interacting with the intracellular C-terminal domain (CTD). In particular, phosphorylation of GluA2 Serine 880 (S880) within the CTD represents a key mechanism to control the internalization of GluA2 containing AMPA-Rs that can undergo subsequent ubiquitination and degradation (21–23) (Fig. 2A). We therefore decided to evaluate through WB the ratio between phosphorylated and total GluA2 levels in Cdkl5 deficient neurons (Fig. 2B and C). Interestingly, Cdkl5 knock-down resulted in a significant increase in S880 phosphorylation ($S880^P$) with respect to control neurons (sh#1: 2.11 ± 0.17, $P = 0.003$; sh#2: 2.27 ± 0.26, $P = 0.0012$) suggesting the presence of an increased intracellular pool of GluA2 containing receptors that might be differently sorted upon internalization. The sorting of internalized GluA2 containing AMPA-Rs towards lysosomal degradation depends on the site-specific ubiquitination of the single subunits (24). To analyse the ubiquitination level of GluA2 in Cdkl5 deficient neurons we performed immunoprecipitation assays with anti-ubiquitin antibodies on lysates of primary hippocampal neurons silenced for Cdkl5 (sh#2) or, as control, with shLacZ and blotted the lysates and immunocomplexes with specific antibodies against GluA2 (Fig. 2D and E). High-molecular-weight forms of GluA2 could be

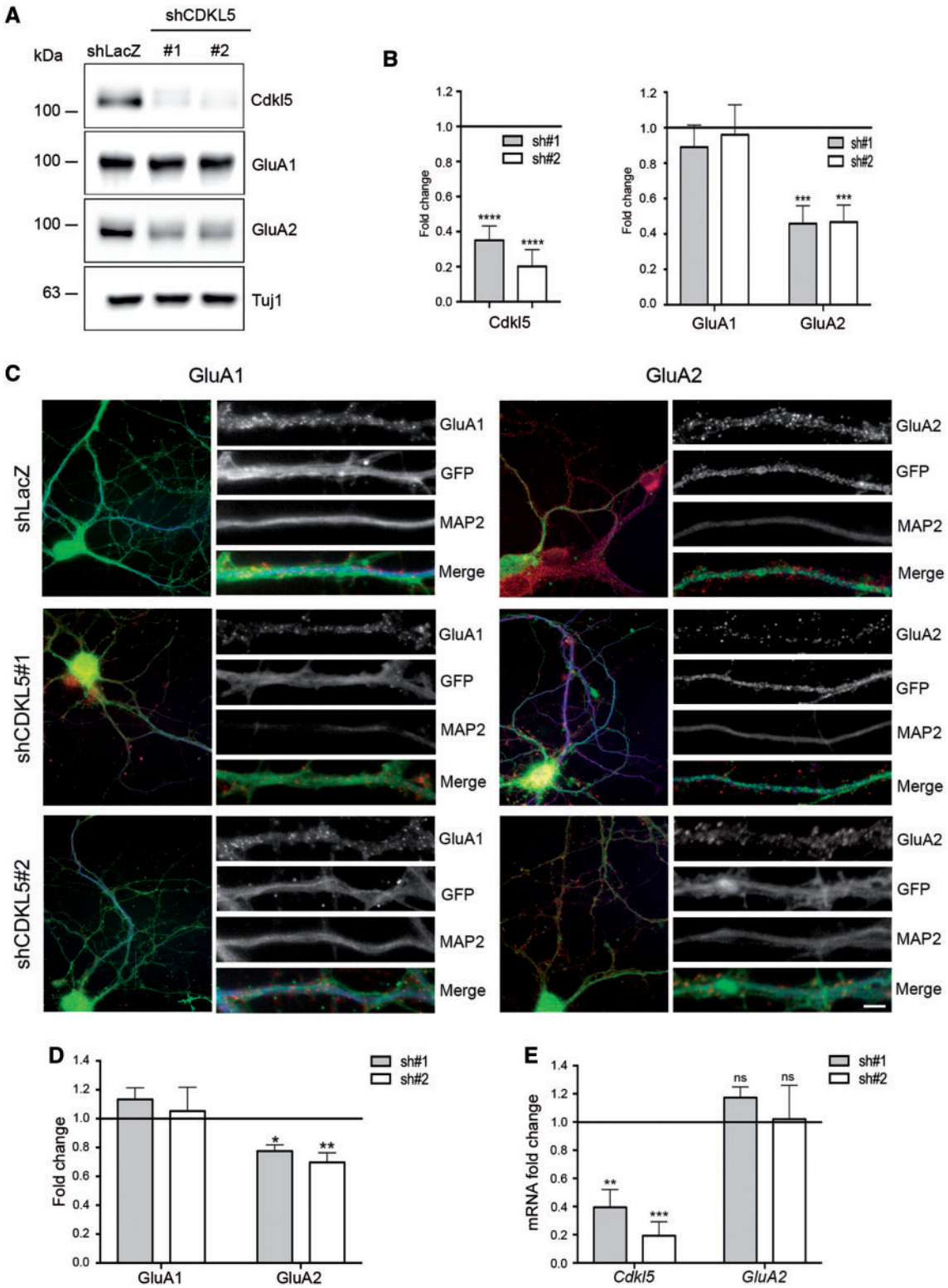

Figure 1. Cdkl5 knock-down affects the expression of AMPA-receptor subunit 2. (**A**) Representative WB showing the expression of Cdkl5, GluA1 and GluA2 in primary hippocampal neurons silenced with shRNAs against Cdkl5 (#1, #2) or, as control, against LacZ. Neurons were silenced at DIV0 and harvested at DIV16–18. Tuj1 was used as loading control. (**B**) Quantification of Cdkl5 (left) and GluA1 and GluA2 (right) expression in neurons silenced for Cdkl5 (sh#1, sh#2). Data are presented as mean ± SEM, $n = 7$ independent experiments. (**C**) Representative images of DIV18 hippocampal neurons silenced with shRNAs against Cdkl5 or LacZ and stained with antibodies against GluA1 or GluA2 (left and right, respectively; red) together with antibodies against GFP (green) and the dendritic marker MAP2 (blue). The white rectangles indicate dendritic regions that are shown at higher magnification with the separate channels showing GFP, GluA1/GluA2, and MAP2. Scale bar, 5 μm. (**D**) Quantification of GluA1 and GluA2 intensity in silenced neurons. Data are presented as mean ± SEM, $n \geq 3$ independent experiments. (**E**) Quantification of *Cdkl5* and *GluA2* mRNA levels in neurons silenced for Cdkl5 (sh#1 and sh#2; DIV16); *Gapdh* was used as internal standard. $n = 4$ independent experiments. Data in B, D and E are presented as fold change compared with the control, shLacZ, indicated with the black line (mean ± SEM). Statistical analysis: One-way ANOVA followed by Dunnetts's multiple comparison test; shCDKL5 versus shLacZ: $^{*}P < 0.05$, $^{**}P < 0.01$, $^{***}P < 0.001$, $^{****}P < 0.0001$.

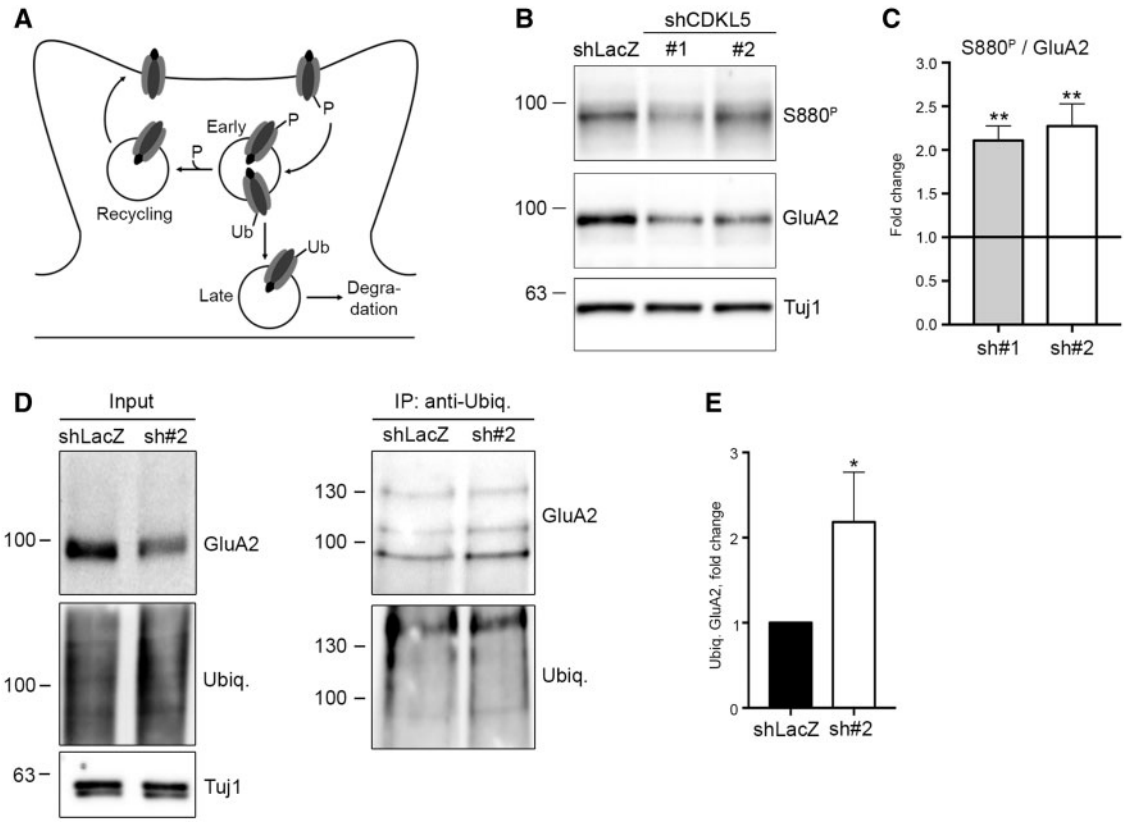

Figure 2. Cdkl5 deficiency causes increased GluA2 phosphorylation and ubiquitin-mediated degradation. (**A**) Schematic representation of GluA2 endosomal trafficking. (**B**) Representative WB showing GluA2 phosphorylated at S880 (S880^P) and its total isoform in primary hippocampal neurons silenced for Cdkl5 expression (#1, #2) using shLacZ as control. Neurons were silenced at DIV0 and harvested at DIV16–18. Tuj1 was used as loading control. (**C**) Graph showing the ratio between S880^P and total GluA2. $n = 4$ independent experiments. Data are presented as fold change compared with the control shLacZ, indicated with the black line (mean ± SEM). Statistical analysis: One-way ANOVA followed by Dunnetts's multiple comparison test; shCdkl5 versus shLacZ: $^{**}P < 0.01$. (**D**) Lysates of silenced hippocampal neurons (DIV15) were immunoprecipitated with anti-ubiquitin antibodies (Ubiq) and the immunocomplexes and the whole cell lysates (Input) were subjected to WB analysis and probed with anti-ubiquitin and anti-GluA2 antibodies. (**E**) Graph showing the quantification of ubiquitinated GluA2 in shLacZ and shCDKL5 treated neurons normalized to the precipitated ubiquitinated proteins and GluA2 levels in the input. Data are presented as mean ± SEM. $^*P < 0.05$; unpaired *t*-test ($n = 3$).

detected in both samples; however, the relative amount of ubiquitinated GluA2 with respect to total GluA2 in the input was significantly increased in Cdkl5 deficient neurons suggesting again that GluA2 is marked for lysosomal degradation in the absence of Cdkl5.

Cdkl5 deficiency impairs AMPA-R surface expression

The above results show that loss of Cdkl5 influences the overall levels of GluA2. However, synaptic transmission is controlled by the number of AMPA-Rs that are exposed at the surface of the synaptic sites and GluA2 in particular plays an important role in regulating Ca^{2+} permeability and currents (25). We therefore found it relevant to analyse the effect of Cdkl5 deficiency on surface bound AMPA-Rs. Neurons silenced with the two Cdkl5 specific shRNAs or the control shLacZ were thus subjected to immunofluorescence analyses under non-permeabilizing conditions using antibodies raised against the extracellular epitopes of GluA1 (Fig. 3A and B) or GluA2 (Fig. 3C and D). Staining for GFP and MAP2 was performed to detect infected neurons and dendritic segments, respectively. The quantification of the signal intensity of surface bound GluA1 (sGluA1) showed a modest but not significant reduction in sGluA1 staining in Cdkl5 silenced neurons (sh#1: 0.92 ± 0.07, $P > 0.05$; sh#2, 0.93 ± 0.09, $P > 0.05$); conversely, a more pronounced and statistically significant decrease was observed of surface bound GluA2 (sh#1: 0.72 ± 0.03, $P = 0.0001$; sh#2, 0.73 ± 0.04, $P = 0.0001$). To get further support of this we used the highly sensitive cell surface biotinylation to label surface exposed AMPA-R subunits; biotinylated proteins were recovered from silenced neurons and analysed by WB in parallel with a fraction of the total cell extracts (Fig. 3E and F). In line with the immunofluorescence studies, Cdkl5 silencing dramatically reduced GluA2 surface expression compared with the control (sh#2: 0.17 ± 0.03, $P < 0.0001$). Interestingly, by means of this sensitive assay we also unmasked a modest deregulation in terms of GluA1 levels (sh#2: 0.57 ± 0.11, $P = 0.0172$). Interestingly, the GluA2/GluA1 ratio was significantly altered in Cdkl5 silenced neurons suggesting that loss of Cdkl5 leads to an altered subunit composition of surface exposed AMPA-Rs (Fig. 3G; sh#2: 0.31 ± 0.06, $P = 0.0004$). These data also combine with results collected by electrophysiology (Fig. 3H–J). Indeed, in order to address functional consequences associated with the absence of Cdkl5, primary hippocampal neurons were acutely silenced for Cdkl5 expression through transfection of a vector expressing shCDKL5#2 and GFP from a bicistronic cassette at DIV10 and the AMPA-R mediated currents quantified at DIV13. This short lasting Cdkl5-silencing allowed us to estimate the contribution of Cdkl5 removal exclusively at the post-synaptic site (GFP positive shRNA expressing neurons) leaving the pre-synaptic compartment normal (untransfected). Under these conditions we found

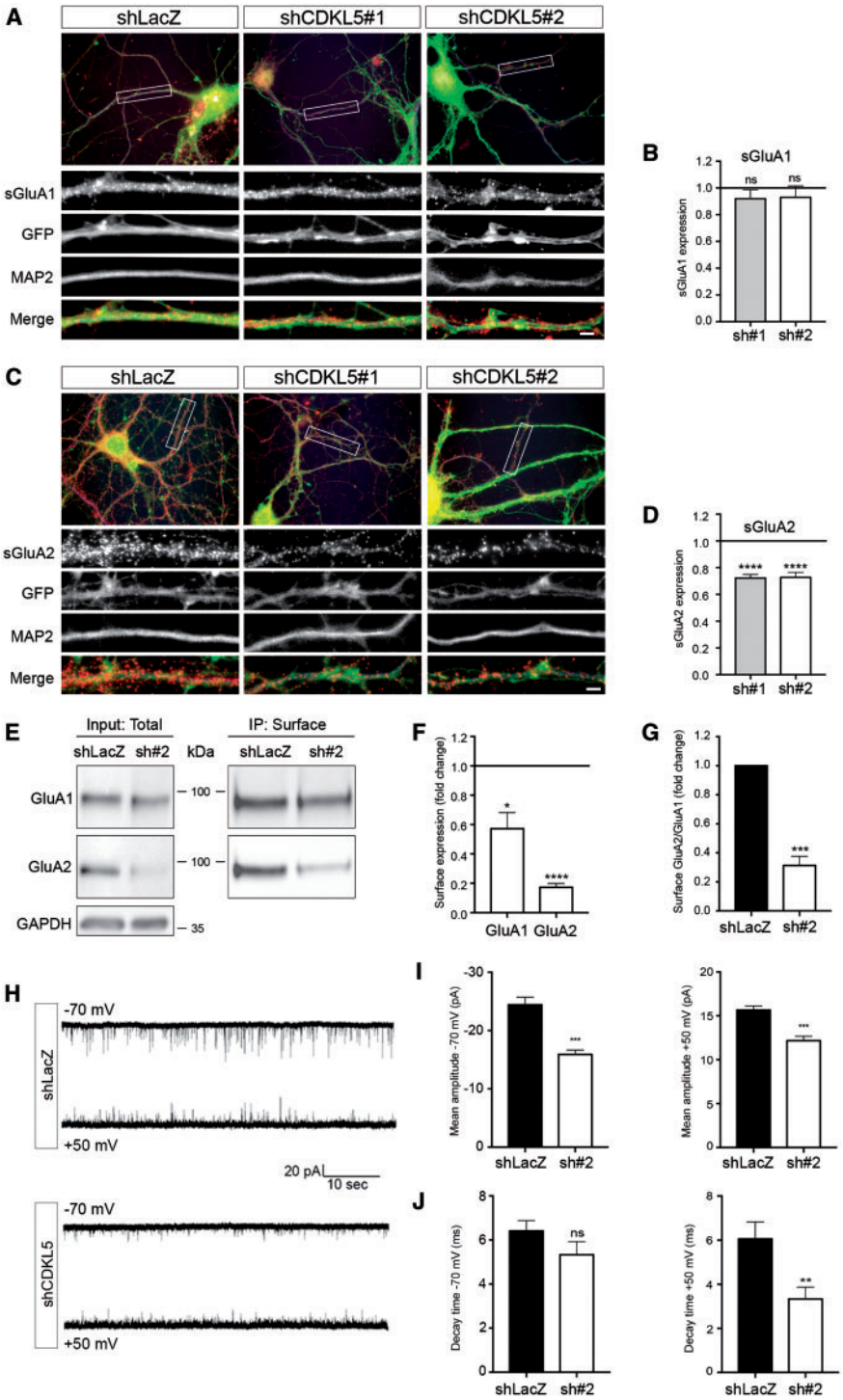

Figure 3. Cdkl5 knock-down impairs membrane exposure of AMPA-Rs. (**A, C**) Representative images of surface staining of GluA1 (sGluA1, panel A, red) or GluA2 [sGluA2, (C), red] of dendritic segments of primary hippocampal neurons (DIV18) silenced for Cdkl5 (sh#1, sh#2) or, as control, for shLacZ. sGluA1 or sGluA2 staining was performed with antibodies raised against the extracellular epitopes under non-permeabilizing conditions where after antibodies against GFP (green) and MAP2 (blue) were used under permeabilizing conditions. The white rectangles indicate dendritic regions that are shown at higher magnification with the separate channels showing GFP, sGluA1/sGluA2, and MAP2. Scale bar, 5 μm. (**B, D**) Graphs showing sGluA1 (B) and sGluA2 (D) immunofluorescence intensities of $MAP2^{+}$ and GFP^{+} dendritic segments. Data are presented as fold change compared with the control shLacZ indicated with the black line. $n > 20$ segments/experiment in ≥ 3 independent experiments (mean ± SEM). Statistical analysis: One-way ANOVA followed by Dunnetts's multiple comparison test; shCdkl5 versus shLacZ: $^{****}P < 0.0001$. (**E**) Representative WB showing GluA1 and GluA2 levels in total extracts (left) or membrane fractions (right) of primary hippocampal neurons (DIV18) silenced for Cdkl5 expression from DIV0 with sh#2 or, as control, with shLacZ. Membrane fractions were purified by biotinylation. GAPDH was used as loading control. (**F**) Quantification of surface expressed GluA1 and GluA2 in neurons silenced for Cdkl5 relative to the control shLacZ, indicated with the black line (mean ± SEM). $n = 3$ independent experiments. Statistical analysis: unpaired *t*-test; sh#2 versus shLacZ: $^{*}P < 0.05$, $^{****}P < 0.0001$. (**G**) Graph showing the ratio of sGluA2/sGluA1 levels silenced neurons. $^{***}P < 0.001$. (**H**) Representative traces of excitatory post-synaptic potentials in miniature (mEPSC) recorded at −70 mV and +50 mV in the two experimental groups. (**I**) Analysis of EPSCs indicates a significant reduction in terms of amplitude for events recorded at both −70 and +50 mV. (**J**) Analysis of EPSCs kinetic properties indicates a reduction in the decay tau for the EPSCs recorded at +50 mV further indicating a decrease in GluA2 containing AMPA-Rs in shCDKL5 neurons with respect to the shLacZ control cells. Data are presented as mean ± SEM. Analyses of $n > 15$ neurons from two independent experiments. Statistical analysis: unpaired *t*-test; sh#2 versus shLacZ: $^{**}P < 0.01$, $^{***}P < 0.001$.

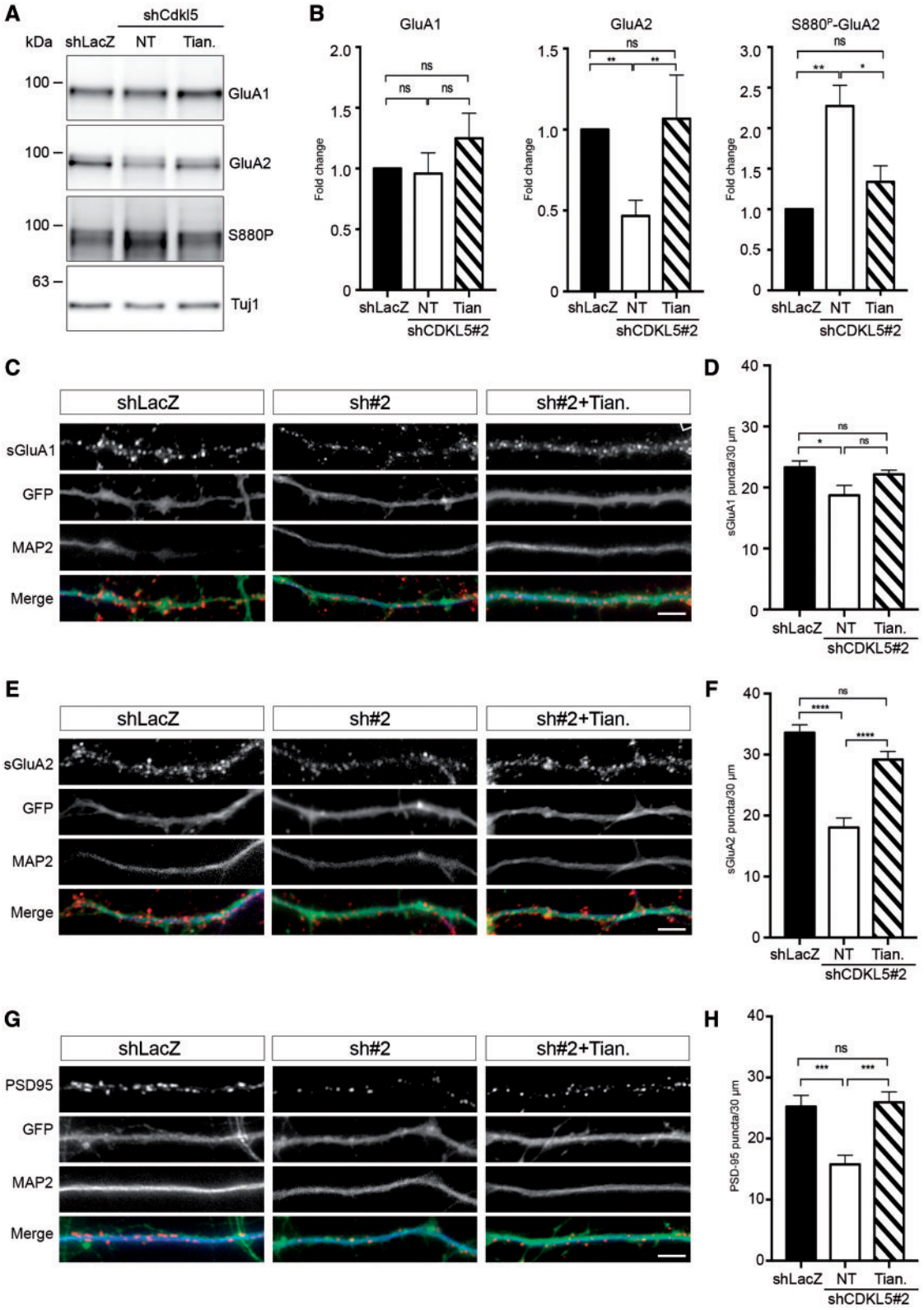

Figure 4. Tianeptine reverts defective GluA2 expression and surfacing in Cdkl5 deficient neurons. (**A**) Representative WB showing levels of GluA1, GluA2 and S880^{P} in neurons silenced from DIV0 with shLacZ or shCDKL5#2 and treated with 10 µM tianeptine from DIV11 to DIV18. Tuj1 was used as loading control. (**B**) Graphs showing the quantification of GluA1, GluA2 and S880^{P} levels in neurons treated like in A. Data are presented as mean ± SEM. $n \geq 3$ independent experiments. Statistical analysis: Tukey's multiple comparisons test; $^{*}P < 0.05$, $^{**}P < 0.01$. (**C, E, G**) Representative images showing sGluA1, sGluA2 and PSD-95 staining, respectively, in dendritic segments of silenced neurons treated or not with tianeptine for 7 days. The separate channels show GFP (green), sGluA1/sGluA2/PSD-95 (red) and MAP2 (blue). Scale bar, 5 µm. (**D, F, H**) Quantification of sGluA1/sGluA2/PSD-95 puncta along 30 µm long GFP^{+} and MAP2^{+} segments. At least 17 segments were counted per condition in 3 independent experiments. Tukey's multiple comparisons test; $^{***}P < 0.001$, $^{****}P < 0.0001$.

by −70 mV patched recordings a significant reduction in the amplitude of excitatory post-synaptic events in miniature (shLacZ 24.43 ± 1.30 pA; sh#2 15.91 ± 0.76 pA, $P = 0.001$) as well as in +50 mV recorded events (shLacZ 15.65 ± 0.47 pA; sh#2 12.18 ± 0.49 pA, $P = 0.001$; Fig. 3H and I). These findings suggest a depletion of both GluA1 and GluA2 receptor subunits in response to the acute Cdkl5 silencing. Interestingly, analysis of kinetics (i.e. rise and decay tau) indicates that events at +50 mV display a reduced decay tau where faster kinetics are typically associated with GluA2-lacking AMPA-Rs (26,27) giving further support to the reduction of GluA2 (−70 mV: shLacZ 6.41± 0.47 ms; sh#2 5.34 ± 0.59 ms; +50 mV: shLacZ 6.06 ± 0.77 ms; sh#2 3.34 ± 0.53 ms, $P = 0.004$) (Fig. 3J). All together, these data confirm a role of Cdkl5 in modulating the expression and surfacing of GluA1/2 containing AMPA-Rs.

Tianeptine restores AMPA-R levels and surface expression in Cdkl5 deficient neurons

Deranged AMPA-R expression has been linked to several neurological disorders including autism and epilepsy and their pharmacologic targeting is considered of high therapeutic relevance (28). Tianeptine is a well-known antidepressant that has been shown to positively influence synaptic plasticity by stabilizing AMPA-Rs at the synaptic sites (20). We therefore found it challenging to test the effect of tianeptine on AMPA-R expression in Cdkl5 silenced neurons and incubated silenced neurons with 10 μM tianeptine for 7 days from DIV11 to DIV18. Intriguingly, overall GluA2 and S880^{P} levels in Cdkl5 deficient neurons were normalized upon exposure to tianeptine and appeared similar to those of control neurons (GluA2: sh#2 0.47 ± 0.10; sh#2 + tia 1.07 ± 0.27; S880^{P}: sh#2 2.27 ± 0.26; sh#2 + tia 1.34 ± 0.20) (Fig. 4A and B). Contrariwise, GluA1 levels were not significantly altered in tianeptine-exposed neurons. To understand whether tianeptine might influence also AMPA-R surfacing we decided to analyse the effect of treatment through the quantification of the number of GluA1 and GluA2 puncta. Such quantification appeared to be quite sensitive and allowed us to confirm the modest effect of Cdkl5 silencing on sGluA1 expression (Fig. 4C and D) whereas, again, sGluA2 expression was strongly influenced (Fig. 4E and F). Importantly, we found that tianeptine was capable of completely restoring the insertion of both AMPA-R subunits into the cell membrane (sGluA1: shLacZ 23.3 ± 1.03; sh#2 18.71 ± 1.63; sh#2 + tian 22.15 ± 0.69; sGluA2: shLacZ 33, 58 ± 1.29; sh#2 18.06 ± 1.55; sh#2 + tian 29.18 ± 1.35). In accordance with previous reports, we observed that neurons deprived of Cdkl5 present less PSD-95 clusters (13,29,30). Interestingly, the capacity of tianeptine to restore GluA2 puncta is accompanied by an increase also in PSD-95 clusters suggesting that this memory-enhancing drug may be capable of promoting spine maturation in Cdkl5 deficient neurons (shLacZ 25.26 ± 1.81; sh#2 15.78 ± 1.49; sh#2 + tian 25.95 ± 1.68).

Discussion

In this study, we characterise a novel role of Cdkl5 in regulating AMPA-R expression. We show that loss of Cdkl5 leads to deranged expression and synaptic insertion of AMPA-Rs in primary cultures of hippocampal neurons. The most remarkable finding of our studies is the dramatic reduction of GluA2 expression, which is accompanied by a more subtle impact on GluA1 levels altogether leading to a net alteration of the specific subunit composition of surface exposed AMPA-Rs.

Cdkl5 influences AMPA-R expression, turnover and functional properties

AMPA-Rs mediate most fast excitatory neurotransmission and the number of AMPA-Rs in the synapses is directly linked to synaptic strength and synapse maturation (31). Synaptic defects associated with the loss of CDKL5 have already been reported in different experimental models such as silenced neurons and *Cdkl5*-null mice but its effect on AMPA-R expression has not been characterized so far (11,13). Several neurological disorders including neurodegenerative and autism-spectrum disorders have been linked to AMPA-R dysfunctions (17–19) and the defective AMPA-R expression caused by CDKL5 deficiency is very likely to contribute to the cognitive defects characterizing CDD patients and mouse models.

Whereas overall GluA1 expression is not significantly reduced in Cdkl5 depleted neurons, we find a strong reduction of GluA2 levels in neuronal lysates and immunostained neurons. As demonstrated through qPCR analyses, GluA2 down-regulation in Cdkl5 deficient neurons is independent of its mRNA expression. Accordingly, we find that Cdkl5 knock-down leads to hyper-phosphorylation of S880 and increased GluA2 ubiquitination. Phosphorylation of S880 is known to be critical in controlling the fate of GluA2 by modulating its affinity for its PDZ-binding partners GRIP1/2 and PICK1 (21,32,33). Specifically, upon PKC-dependent phosphorylation at S880, the affinity of GluA2 for GRIP1/2, which stabilises the surface expression of GluA2-containing receptors, is lost in favour of PICK1-binding that drives the receptor towards internalization in non-recycling compartments and/or towards lysosomal ubiquitin-dependent degradation. Alternatively, internalized GluA2 can be dephosphorylated by PP1 and/or deubiquitinated and redirected back towards the cell surface (22,23). The higher level of GluA2 S880^{P} and ubiquitination in Cdkl5 depleted neurons is indicative of an increased intracellular retention and subsequent lysosomal degradation of GluA2 containing AMPA-Rs that justifies the strong reduction in total GluA2 expression. How loss of Cdkl5 leads to increased GluA2 phosphorylation and ubiquitination is not clear: a role of CDKL5 in modulating PKC and/or PP1 activities as well as the ubiquitination system has not been described and the putative ubiquitin ligase that controls GluA2 ubiquitination has not yet been identified (23). The only link so far reported between CDKL5 and ubiquitin is the ubiquitin ligase Mind Bomb 1 (Mib1) that was found to interact with CDKL5 regulating its levels and subcellular localization (41).

Not surprisingly, the dramatic reduction in overall GluA2 levels is also reflected at the plasma membrane where surface exposed GluA2 levels are diminished. Interestingly, by means of a surface biotinylation assay and through the quantification of sGluA1 puncta, we could also detect a less pronounced but significant reduction in surface exposed GluA1. Surfacing and internalization of AMPA-Rs are regulated by subunit-specific rules that are mainly determined by the interaction of the distinct C-terminal tails with specific proteins. According to these rules, GluA1 mediates the synaptic delivery of heteromeric GluA1/GluA2 receptors whereas GluA2 governs their internalization (34). It is thus plausible that the dramatic reduction of GluA2 influences GluA1 surface levels to some extent, even though we cannot rule out that CDKL5 deficiency may affect

GluA1 surfacing independently of its effect on GluA2. Our findings are further corroborated by a significant reduction in the amplitude of AMPA-R mediated mEPSCs recorded at both −70 and +50 mV. Interestingly, our electrophysiological results show a stronger impact of Cdkl5 deficiency on GluA2 containing AMPA-Rs as indicated by the kinetic properties of mEPSCs events at +50 mV. All together, these results indicate that silencing of Cdkl5 leads to an unbalanced expression of synaptic AMPA-Rs towards a GluA2 lacking calcium-permeable form.

Implications of Cdkl5-dependent unbalance of AMPA-R

The specific subunit composition is critical for AMPA-R function. In particular, thanks to RNA-editing of the *GluA2* mRNA, AMPA-Rs containing GluA2 are Ca^{2+} impermeable (CI) and with a linear current-voltage relationship whereas those devoid of GluA2 are Ca^{2+} permeable (CP) (35). The dramatic depletion of GluA2 that we observe in Cdkl5 silenced neurons is thus expected to alter significantly calcium homeostasis in excitatory spines. Calcium conductance in these spines may thus be increased and, consequently, lead to an unhampered and detrimental calcium entry influencing intracellular signalling pathways. Of note, kinome profiling studies revealed an altered activity of kinases involved in synaptic plasticity (i.e. PKC, PKA, and protein kinase D) (4). Further studies are needed to clarify whether there is a functional link between these data.

An unbalanced subunit composition of AMPA-R composition at the PSD may have important implications also for LTP. Indeed, during LTP induction (early phase) there is a rapid and transient incorporation of GluA2-lacking AMPA-Rs whilst the maintenance (late phase) requires the insertion of GluA2-containing receptors at the synaptic sites (36). The apparent impairment of Cdkl5 deficient neurons in stabilizing GluA2 containing receptors at the PSD may thus affect the late phase of LTP. Accordingly, while LTP induction was not diminished in cortical slices of *Cdkl5*-null mice, its maintenance was compromised (13).

Interestingly, overexpression and silencing studies have demonstrated a specific and direct correlation between the presence of GluA2 containing AMPA-Rs at synaptic sites and the formation and maturation of dendritic spines (37). Similarly, even if conflicting data exist, most data converge on a role of Cdkl5 in promoting dendritic spine maturation and their stability. Indeed, loss of Cdkl5 causes an increased number of immature dendritic spines, which is accompanied by reduced number of PSD-95 and Homer clusters, reduced dendritic spine stabilization, defective excitatory activity and impaired LTP (11–13,30). In line with these studies we also observe in our experimental model a reduced number of PSD-95 puncta upon silencing of Cdkl5. It is thus tempting to speculate that Cdkl5 may influence PSD-95 clusters and spine maturation through its strong influence on GluA2 expression. On the other hand, it should be kept in mind that PSD-95 acts as a key regulator of synaptic plasticity by stabilizing AMPA-Rs at the synaptic site through its interaction with the stargazine/TARP proteins (38); this raises the possibility that a Cdkl5 dependent deregulation of PSD-95 could lead to the observed AMPA-R defects. Previous reports have established a functional link between PSD-95 and Cdkl5. The interaction of Cdkl5 with palmitoylated PSD-95 was suggested to anchor this kinase at the synaptic sites whereas Cdkl5-mediated phosphorylation of NGL-1 was found to promote the PSD-95/NGL-1 interaction (11,12). A further comprehension of the direct interactors and phosphorylation substrates of Cdkl5 in dendritic spines is still needed to improve our understanding of the primary defect(s) leading to the severe derangement of the glutamatergic post-synaptic machinery characterizing neurons devoid of Cdkl5. Such knowledge is particularly important for revealing effective druggable targets and designing new successful therapeutic strategies. The presence of Cdkl5 in dendritic spines and the fact that its local synthesis and degradation are finely tuned in an activity-dependent manner (10) suggest that it may directly target and regulate various post-synaptic proteins.

Tianeptine efficiently reverts Cdkl5-dependent spine defects

The pharmacological targeting of AMPA-Rs constitutes an important goal for various neurological disorders (28). On that basis, we focused our attention on tianeptine, an antidepressant with structural similarities to the tricyclic antidepressant agents but with different pharmacological properties (39). Extensive studies revealed that tianeptine has no significant binding affinity for classical anti-depressant drug-directed targets (i.e. 5-HT receptors, dopamine receptors, adrenoceptor, glutamate receptors and monoamine transporters) (40) even if it has been reported to act as an agonist of the μ-opoid receptor (MOR; 42). Tianeptine appears to exert its therapeutic action by modulating glutamatergic neurotransmission. Specifically, tianeptine can potentiate AMPA-R signalling by activating CaMKII and PKA via the p38, p42/44 MAPK and JNK pathways, and by increasing the phosphorylation of GluA1 at serine-831 and -845 (43). Moreover, tianeptine can regulate the trafficking and synaptic content of AMPA-Rs through a CaMKII- and stargazin-dependent mechanism that requires the phosphorylation of stargazin and the interaction of the AMPA-R/stargazin complex with PDZ scaffold proteins such as PSD-95 (20). At the molecular level, phosphorylation of stargazin promotes the stargazin/PSD-95 interaction, which in turn recruits and immobilizes AMPA-Rs at post-synaptic sites (44). Functionally, electrophysiological studies showed that tianeptine increases excitatory post-synaptic currents in hippocampal neurons (45) and reverses stress-induced impairment of LTP (46).

Interestingly, we found that tianeptine treatment rescued GluA2 expression in Cdkl5 silenced neurons. Even though the underlying molecular mechanisms are still unknown, we hypothesize that this increase may rely on an increased synaptic retention of GluA2 containing AMPA-Rs that would otherwise be internalized and degraded. This model is in agreement with the concomitant decrease of S880 phosphorylation that we observed in tianeptine treated neurons. Importantly, besides rescuing the overall levels of GluA2, we also found that tianeptine normalized the number of GluA2 and PSD-95 puncta, suggesting that this drug may have an overall positive effect promoting dendritic spine maturation and synaptic activity in Cdkl5 deficient neurons. Considering that tianeptine acts as a MOR agonist it is worth mentioning that other MOR agonists, such as morphine, have been reported to promote AMPA-R internalization (47). We thus consider likely that the tianeptine-mediated effect on *Cdkl5* deficient neurons is MOR independent.

Tianeptine possesses a unique pharmacological profile that makes it an interesting drug for various neurological disorders. The drug has been used as an antidepressant for over 30 years and its outstanding clinical tolerance is well known (48). In addition to its antidepressant effects, clinical benefit was demonstrated with tianeptine improving cognitive performance in cognitively impaired depressed patients (49,50). Of relevance,

notwithstanding its effect in facilitating AMPA-R signalling, tianeptine was not found to increase seizure frequency when tested in epileptic patients (51). Moreover, tianeptine has also been found to have neuroprotective effects in part by down-regulating calpain, a Ca^{2+}-activated protease that causes the degradation of various synaptic proteins (52,53). Recently, tianeptine was found capable of improving the respiration phenotype in a mouse model of Rett syndrome (54) and, based on our findings, we propose that future studies should be undertaken to test the therapeutic potential of tianeptine for CDD.

Materials and Methods

Ethical statement

Protocols and use of animals were approved by the Animal Ethics Committee of the University of Insubria and in accordance with the guidelines released by the Italian Ministry of Health. Adult mice were euthanized by cervical dislocation, while neonates were sacrificed by exposure to CO_2 followed by decapitation.

Antibodies and reagents

CDKL5 (Sigma Aldrich, HPA002847; Santa Cruz Biotechnology, sc376314), GAPDH (Sigma Aldrich, G9545), GFP (Millipore AB16901), GluA1 (Abcam, ab86141; Calbiochem, PC246), GluA2 (Millipore, MAB397), GluA2-S880P (Biorbyt, orb256572), MAP2 (Abcam mouse, ab11267; Abcam rabbit, ab32454), PSD-95 (Thermo Fischer Scientific, MA1045), Tuj1 (Covance, MMS-435P), Ubiquitin (Santa Cruz Biotechnology, sc-8017). HRP-conjugated goat anti-mouse or anti-rabbit secondary Abs for immunoblotting and secondary Alexa Fluor anti-rabbit and anti-mouse Abs for immunofluorescence were purchased from Thermo Fischer Scientific. Strychnine was purchased from Sigma Aldrich and tianeptine (7-[(3-chloro-6-methyl-5, 5-dioxo-11H-benzo[c][2, 1] benzothiazepin-11-yl)amino]heptanoic acid, sodium salt), tetradotoxin (TTX), D-(−)-2-Amino-5-phosphonopentanoic acid (APV), and bicuculline were all purchased from Tocris.

Primary neuronal cultures

Primary hippocampal cultures were prepared as described previously (9). Silencing of Cdkl5 expression was obtained infecting neurons 5 h after plating. Recombinant lentiviruses were produced as described elsewhere (55); the Cdkl5 targeting sequences were shCDKL5#1: CTATGGAGTTGTACTTAA, shCDKL5#2: GTGAGAGCGAAAGGCCTT. A shLacZ construct directed against β-galactosidase was used as control.

Pharmacological treatments

Tianepetine treatment of primary hippocampal neurons was performed from DIV11 adding the drug to the conditioned medium at the final concentration of 10 μM and replenished every second day till DIV18 when neurons were harvested for further analysis.

Real time PCR

Total RNA was isolated from primary hippocampal neurons (DIV18) using TRIzol Reagent (Life Technologies) according to the manufacturer's instructions. cDNA was synthesized from 500 ng of RNA using iScript Select cDNA Synthesis Kit (Bio-Rad) and 1/20th of the reverse transcription reaction was used for quantitative real-time PCR using SYBR Select Master Mix (Applied Biosystems) and a BioRad/MJ Research Chromo4 real-time cycler. Each sample was assayed in triplicate. The data were analysed using the ΔΔCt method. A melting curve was automatically generated for each sample and confirmed that a single amplicon was generated in each reaction. Primers were: *Cdkl5:* forw. TTCCCAGCTGTTAACCATCC; rev. AAGGAGACCGG TCCAAAAGT; *GluA2:* forw. AAGGAGGAAAGGGAAACGAG, rev. CCGAAGTGGAAAACTGAACC; *Gapdh:* forw. ATTGTCAGCAATGC ATCCTG, rev. ATGGACTGTGGTCATGAGCC.

Western blotting

Primary neurons were lysed directly in Laemmli buffer and a volume corresponding to approximately 10 μg of proteins was separated by 8–10% SDS-PAGE.

Immunoprecpitation

Primary neurons were harvested in ice-cold PBS containing 10 mM N-ethylmaleimide (NEM), then centrifuged at 100*g* for 15 min at 4°C. The resulting pellet was lysed in ice-cold RIPA-buffer (150 mM NaCl, 1% Triton X-100, 0, 5% deoxycholate, 0, 1% SDS, 5 mM EDTA, 20 mM Tris–HCl pH 7.4) supplemented with protease inhibitor cocktail (Sigma Aldrich) and 10 mM NEM. The soluble fraction was cleared by centrifugation and the protein content of the supernatant was evaluated using the BCA Protein Assay (Thermo Fisher Scientific). Cell lysates corresponding to 250 μg of protein were mixed with 3 μg of anti-ubiquitin antibody and 30 μl of slurry protein A/G PLUS-agarose (Santa Cruz Biotechnology) and incubated overnight at 4°C.

Cell surface biotinylation

Primary neurons were washed with HBSS-glucose (1%) and incubated with EZ-link sulfo-NHS-SS-Biotin (Thermo Fisher Scientific) (0.75 mg/ml in HBSS-glucose) for 25 min at 4°C. Unreacted biotin quenched with 1% BSA/HBSS-glucose for 10 min at 4°C. After washing, the neurons were lysed in RIPA-buffer (50 mM Tris–HCl pH8, 150 mM NaCl, 1 mM EDTA, 1% Triton X-100, 1% sodium-deocycholate, 0.1% SDS supplemented with protease inhibitor cocktail (Sigma Aldrich) for 1 h at 4°C on a rotating wheel. A 200 μg of clarified lysates were incubated with UltraLink Streptavidin beads (Thermo Fisher Scientific) in RIPA-buffer for 2 h at 4°C and cell-surface biotinylated proteins recovered by centrifugation, washed in RIPA-buffer and analysed by WB.

Immunofluorescence

Primary hippocampal neurons plated on glass coverslips were fixed with 4% paraformaldehyde/PBS with 4% saccharose at DIV15–18 for 15 min and incubated with blocking solution (PBS, 5% horse serum, 0.2% Triton X-100) for 1 h. The addition of 0.2% Triton X-100 was omitted for the staining of surface-expressed GluA1 and GluA2. Incubation with primary Abs was performed over night at 4°C in a humidified chamber; after washing in PBS neurons were incubated with secondary Abs for 1 h at room temperature. Coverslips were mounted with ProLong Gold antifade reagent (Molecular Probes) and images captured at an Olympus BX51 Fluorescence microscope equipped with Retiga

R1 (QImaging) CCD camera. Fluorescence quantifications were performed with Image J software.

In vitro electrophysiology

Recordings of excitatory post-synaptic potentials in miniature (mEPSCs) were recorded clamping the voltage at −70 mV and + 50 mV at room temperature (20–25°C) in the presence of the following drugs: 1 μM TTX, 10 μM bicuculline, 100 μM APV and 1 μM strychnine. Whole-cell voltage clamp recordings were obtained using the Multiclamp 700A amplifier (Molecular Devices) and pClamp-10 software (Axon Instruments, Foster City, CA, USA). All experiments were performed with DIV13 cultured primary hippocampal neurons. Currents were filtered at 2–5 kHz, sampled above 5 kHz and analysed (off-line) with Clampfit-pClamp 10.2 software. External solutions contained 125 mM NaCl, 5 mM KCl, 1.2 mM $MgSO_4$, 1.2 mM KH_2PO_4, 2 mM $CaCl_2$, 6 mM D-glucose, and 25 mM HEPES/NaOH with pH 7.4. Recording pipettes were fabricated from capillary glass using a two-stage puller (Narishige, Japan), had tip resistances of 5–6 MΩ and were filled with the intracellular solution containing: 130 mM CsGluconate, 8 mM CsCl, 2 mM NaCl, 10 mM HEPES, 4 mM EGTA, 4 mM MgATP and 0.3 mM Tris–GTP, pH 7.4. Series resistance was monitored during experiments, and recordings with changes over 20% control during experiments were rejected.

Statistical analyses

All values are expressed as the mean ± SEM. The significance of results was evaluated by Student's *t*-test, one-way ANOVA followed by Dunnett's or Tuckey's multiple comparison test when appropriate.

Supplementary Material

Supplementary Material is available at *HMG* online.

Conflict of Interest statement. T.G. is a shareholder of Healx Ltd; D.C. is a shareholder of Healx Ltd and Numedicus Ltd.

Funding

This work was funded by the Italian CDKL5 parent's association l'Albero di Greta, by the Telethon Foundation #GGP15098 (C.K.N.) and by a research grant from the University of Pennsylvania Orphan Disease Center on behalf of Loulou Foundation (C.K.N.). The financial support of the Fondazione Telethon-Italy Grant #GGP16015 (to F.A.) is acknowledged.

References

1. Kilstrup-Nielsen, C., Rusconi, L., La Montanara, P., Ciceri, D., Bergo, A., Bedogni, F. and Landsberger, N. (2012) What we know and would like to know about CDKL5 and its involvement in epileptic encephalopathy. *Neural. Plast.*, **2012**, 728267.
2. Fehr, S., Wilson, M., Downs, J., Williams, S., Murgia, A., Sartori, S., Vecchi, M., Ho, G., Polli, R., Psoni, S. *et al.* (2013) The CDKL5 disorder is an independent clinical entity associated with early-onset encephalopathy. *Eur. J. Hum. Genet.*, **21**, 266–273.
3. Zhou, A., Han, S. and Zhou, Z.J. (2017) Molecular and genetic insights into an infantile epileptic encephalopathy – CDKL5 disorder. *Front. Biol.*, **12**, 1–6.
4. Wang, I.T., Allen, M., Goffin, D., Zhu, X., Fairless, A.H., Brodkin, E.S., Siegel, S.J., Marsh, E.D., Blendy, J.A. and Zhou, Z. (2012) Loss of CDKL5 disrupts kinome profile and eventrelated potentials leading to autistic-like phenotypes in mice. *Proc. Natl. Acad. Sci. USA*, **109**, 21516–21521.
5. Amendola, E., Zhan, Y., Mattucci, C., Castroflorio, E., Calcagno, E., Fuchs, C., Lonetti, C., Silingardi, D., Vyssotski, A.L., Farley, D. *et al.* (2014) Mapping pathological phenotypes in a mouse model of CDKL5 disorder. *PLoS One*, **9**, e91613.
6. Jhang, C.L., Huang, T.N., Hsueh, Y.P. and Liao, W. (2017) Mice lacking cyclin-dependent kinase-like 5 manifest autistic and ADHD-like behaviors. *Hum. Mol. Genet.*, **26**, 3922–3934.
7. Okuda, K., Kobayashi, S., Fukaya, M., Watanabe, A., Murakami, T., Hagiwara, M., Sato, T., Ueno, H., Ogonuki, N., Komano-Inoue, S., *et al.* (2017) CDKL5 controls postsynaptic localization of GluN2B NMDA receptors in the hippocampus and regulates seizure susceptibility. *Neurobiol. Dis.*, **106**, 158–170.
8. Rusconi, L., Salvatoni, L., Giudici, L., Bertani, I., Kilstrup-Nielsen, C., Broccoli, V. and Landsberger, N. (2008) CDKL5 expression is modulated during neuronal development and its subcellular distribution is tightly regulated by the C-terminal tail. *J. Biol. Chem.*, **283**, 30101–30111.
9. Rusconi, L., Kilstrup-Nielsen, C. and Landsberger, N. (2011) Extrasynaptic N-methyl-D-aspartate (NMDA) receptor stimulation induces cytoplasmic translocation of the CDKL5 kinase and its proteasomal degradation. *J. Biol. Chem.*, **286**, 36550–36558.
10. La Montanara, P., Rusconi, L., Locarno, A., Forti, L., Barbiero, I., Chandola, C., Kilstrup-Nielsen, C. and Landsberger, N. (2015) Synaptic synthesis, dephosphorylation and degradation: a novel paradigm for a developmentally regulated NMDA-dependent control of CDKL5. *J. Biol. Chem.*, **290**, 4512–4527.
11. Ricciardi, S., Ungaro, F., Hambrock, M., Rademacher, N., Stefanelli, G., Brambilla, D., Sessa, A., Magagnotti, C., Bachi, A., Giarda, E. *et al.* (2012) CDKL5 ensures excitatory synapse stability by reinforcing NGL-1-PSD95 interaction in the postsynaptic compartment and is impaired in patient iPSC-derived neurons. *Nat. Cell. Biol.*, **14**, 911–923.
12. Zhu, Y.-C., Li, D., Wang, L., Lu, B., Zheng, J., Zhao, S.-L., Zeng, R. and Xiong, Z.-Q. (2013) Palmitoylation-dependent CDKL5-PSD-95 interaction regulates synaptic targeting of CDKL5 and dendritic spine development. *Proc. Natl. Acad. Sci. USA*, **110**, 9118–9123.
13. Della Sala, G., Putignano, E., Chelini, G., Melani, R., Calcagno, E., Ratto, M.G., Amendola, E., Gross, C.T., Giustetto, M. and Pizzorusso, T. (2016) Dendritic spine instability in a mouse model of CDKL5 disorder is rescued by insulin-like growth factor 1. *Biol. Psychiatry*, **80**, 302–311.
14. Henley, J.M. and Wilkinson, K.A. (2016) Synaptic AMPA receptor composition in development, plasticity and disease. *Nat. Rev. Neurosci.*, **17**, 337–350.
15. Wu, Y., Arai, A.C., Rumbaugh, G., Srivastava, A.K., Turner, G., Hayashi, T., Suzuki, E., Jiang, Y., Zhang, L., Rodriguez, J. *et al.* (2007) Mutations in ionotropic AMPA receptor 3 alter channel properties and are associated with moderate cognitive impairment in humans. *Proc. Natl. Acad. Sci. USA*, **104**, 18163–18168.
16. Zhao, W.Q., Santini, F., Breese, R., Ross, D., Zhang, X.D., Stone, D.J., Ferrer, M., Townsend, M., Wolfe, A.L., Seager, M.A., *et al.*

(2010) Inhibition of calcineurin-mediated endocytosis and alpha-amino-3-hydroxy-5-methyl-4-isoxazolepropionic acid (AMPA) receptors prevents amyloid beta oligomer-induced synaptic disruption. *J. Biol. Chem.*, **285**, 7619–7632.
17. Mignogna, M.L., Giannandrea, M., Gurgone, A., Fanelli, F., Raimondi, F., Mapelli, L., Bassani, S., Fang, H., Van Anken, E., Alessio, M., *et al.* (2015) The intellectual disability protein RAB39B selectively regulates GluA2 trafficking to determine synaptic AMPAR composition. *Nat. Commun.*, **6**, 6504.
18. Li, W., Xu, X. and Pozzo-Miller, L. (2016) Excitatory synapses are stronger in the hippocampus of Rett syndrome mice due to altered synaptic trafficking of AMPA-type glutamate receptors. *Proc. Natl. Acad. Sci. USA*, **113**, E1575–E1584.
19. Volk, L., Chiu, S.L., Sharma, K. and Huganir, R.L. (2015) Glutamate synapses in human cognitive disorders. *Annu. Rev. Neurosci.*, **38**, 127–149.
20. Zhang, H., Etherington, L.A., Hafner, A.S., Belelli, D., Coussen, F., Delagrange, P., Chaouloff, F., Spedding, M., Lambert, J.J., Choquet, D., Groc, L. (2013) Regulation of AMPA receptor surface trafficking and synaptic plasticity by a cognitive enhancer and antidepressant molecule. *Mol. Psychiatry.*, **18**, 471–484.
21. Matsuda, S., Mikawa, S. and Hirai, H. (2002) Phosphorylation of serine-880 in GluR2 by protein kinase C prevents its C terminus from binding with glutamate receptor-interacting protein. *J. Neurochem.*, **73**, 1765–1768.
22. Goo, M.S., Scudder, S.L. and Patrick, G.N. (2015) Ubiquitin-dependent trafficking and turnover of ionotropic glutamate receptors. *Front. Mol. Neurosci.*, **8**, 60.
23. Lussier, M.P., Nasu-Nishimura, Y. and Roche, K.W. (2011) Activity-dependent ubiquitination of the AMPA receptor subunit GluA2. *J. Neurosci.*, **31**, 3077–3081.
24. Widagdo, J., Chai, Y.J., Ridder, M.C., Chau, Y.Q., Johnson, R.C., Sah, P., Huganir, R.L. and Anggono, V. (2015) Activity-dependent ubiquitination of GluA1 and GluA2 regulates AMPA receptor intracellular sorting and degradation. *Cell Rep.*, **10**, 783–795.
25. Bassani, S., Valnegri, P., Beretta, F. and Passafaro, M. (2009) The GluR2 subunit of AMPA receptors: synaptic role. *Neuroscience*, **158**, 55–61.
26. Mosbacher, J., Schoepfer, R., Monyer, H., Burnashev, N., Seeburg, P.H. and Ruppersberg, J.P. (1994) A molecular determinant for submillisecond desensitization in glutamate receptors. *Science*, **266**, 1059–1062.
27. Thiagarajan, T.C., Lindskog, M. and Tsien, R.W. (2005) Adaptation to synaptic inactivity in hippocampal neurons. *Neuron*. **47**, 725–737.
28. Lee, K., Goodman, L., Fourie, C., Schenk, S., Leitch, B. and Montgomery, J.M. (2015) AMPA receptors as therapeutic targets for neurological disorders. *Adv. Protein Chem. Struct. Biol.*, **103**, 203–261.
29. Trazzi, S., Fuchs, C., Viggiano, R., De Franceschi, M., Valli, E., Jedynak, P., Hansen, F.K., Perini, G., Rimondini, R., Kurz, T. *et al.* (2016) HDAC4: a key factor underlying brain development alterations in CDKL5 disorder. *Hum. Mol. Genet.*, **25**, 3887–3907.
30. Pizzo, R., Gurgone, A., Castroflorio, E., Amendola, E., Gross, C., Sassoè-Pognetto, M. and Giustetto, M. (2016) Lack of Cdkl5 Disrupts the Organization of Excitatory and Inhibitory Synapses and parvalbumin interneurons in the primary visual cortex. *Front. Cell. Neurosci.*, **10**, 261.
31. Bassani, S., Folci, A., Zapata, J. and Passafaro, M. (2013) AMPAR trafficking in synapse maturation and plasticity. *Cell. Mol. Life Sci.*, **70**, 4411–4430.
32. Chung, H.J., Xia, J., Scannevin, R.H., Zhang, X. and Huganir, R.L. (2000) Phosphorylation of the AMPA receptor subunit GluR2 differentially regulates its interaction with the PDZ domain-containing proteins. *J. Neurosci.*, **20**, 7258–7267.
33. Perez, J.L., Khatri, L., Chang, C., Srivastava, S., Osten, P. and Ziff, E.B. (2001) PICK1 targets activated protein kinase Calpha to AMPA receptor clusters in spines of hippocampal neurons and reduces surface levels of the AMPA-type glutamate receptor subunit 2. *J. Neurosci.*, **21**, 5417–5428.
34. Lee, S.H., Simonetta, A. and Sheng, M. (2004) Subunit rules governing the sorting of internalized AMPA receptors in hippocampal neurons. *Neuron* **43**, 221–236.
35. Isaac, J.T., Ashby, M.C. and McBain, C.J. (2007) The role of the GluR2 subunit in AMPA receptor function and synaptic plasticity. *Neuron*, **54**, 859–871.
36. Liu, S.Q. and Cull-Candy, S.G. (2000) Synaptic activity at calcium-permeable AMPA receptors induces a switch in receptor subtype. *Nature*, **405**, 454–458.
37. Saglietti, L., Dequidt, C., Kamieniarz, K., Rousset, M.C., Valnegri, P., Thoumine, O., Beretta, F., Fagni, L., Choquet, D., Sala, C. *et al*, M. (2007) Extracellular interactions between GluR2 and N-cadherin in spine regulation. *Neuron*, **54**, 461–477.
38. Coley, A.A. and Gao, W.J. (2017) PSD95: a synaptic protein implicated in schizophrenia or autism? *Prog. Neurpsychopharmacol. Biol. Psychiatry*, S0278–5846, 30658–30659.
39. McEwen, B.S., Chattarji, S., Diamond, D.M., Jay, T.M., Reagan, L.P., Svenningsson, P. and Fuchs, E. (2010) The neurobiological properties of tianeptine (Stablon): from monoamine hypothesis to glutamatergic modulation. *Mol. Psychiatry*, **15**, 237–249.
40. Svenningsson, P., Bateup, H., Qi, H., Takamiya, K., Huganir, R.L., Spedding, M., Roth, B.L., McEwen, B.S. and Greengard, P. (2007) Involvement of AMPA receptor phosphorylation in antidepressant actions with special reference to tianeptine. *Eur. J. Neurosci.*, **26**, 3509–3517.
41. Mertz, J., Tan, H., Pagala, V., Bai, B., Chen, P.-C., Li, Y., Cho, J.-H., Shaw, T., Wang, X. and Peng, J. (2015) Sequential elution interactome analysis of the Mind Bomb 1 Ubiquitin Ligase reveals a novel role in dendritic spine outgrowth. *Mol. Cell. Proteom.*, **14**, 1898–1910.
42. Gassaway, M.M., Rives, M.-L., Kruegel, A.C., Javitch, J.A. and Sames, D. (2014) The antidepressant and neurorestorative agent tianeptine is a μ-opoid receptor agonist. *Transl. Psyciatry*, **4**, e411.
43. Szegedi, V., Juhász, G., Zhang, X., Barkóczi, B., Qi, H., Madeira, A., Kapus, G., Svenningsson, P., Spedding, M. and Penke, B. (2011) Tianeptine potentiates AMPA receptors by activating CaMKII and PKA via the p38, p42/44 MAPK and JNK pathways. *Neurochem. Int.*, **59**, 1109–1122.
44. Choi, J., Ko, J., Park, E., Lee, J.R., Yoon, J., Lim, S. and Kim, E. (2002) Phosphorylation of stargazin by protein kinase A regulates its interaction with PSD-95. *J. Biol. Chem.*, **277**, 12359–12363.
45. Kole, M. H. P., Swan, L. and Fuchs, E. (2002) The antidepressant tianeptine persistently modulates glutamate receptor currents of the hippocampal CA3 commissural associational synapse in chronically stressed rats. *Eur. J. Neurosci.*, **16**, 807–816.
46. Qi, H., Mailliet, F., Spedding, M., Rocher, C., Zhang, X., Delagrange, P., McEwen, B., Jay, T.M. and Svenningsson, P. (2009) Antidepressants reverse the attenuation of the neurotrophic MEK/MAPK cascade in frontal cortex by elevated platform stress; reversal of effects on LTP is associated with GluA1 phosphorylation. *Neuropharmacology*, **56**, 37–46.
47. Kam, A.Y., Liao, D., Loh, H.H. and Law, P.Y. (2010) Morphine induces AMPA receptor internalization in primary

hippocampal neurons via calcineurin-dependent dephosphorylation of GluR1 subunits. *J. Neurosci.*, **30**, 15304–15316.
48. Wilde, M.I. and Benfield, P. (1995) Tianeptine. A review of its pharmacodynamics and pharmacokinetic properties, and therapeutic efficacy in depression and coexisting anxiety and depression. *Drugs*, **49**, 411–439.
49. Karpukhin, I.B. (2008) Use of Coaxil (tianeptine) in elderly patients with combined mild cognitive and depressive-anxiety disorders. *Neurosci. Behav. Phys.* **39**, 53–56.
50. Klasik, A., Krysta, K. and Krupka-Matuszczyk, I. (2011) Effect of tianeptine on cognitive functions in patients with depressive disorders during a 3-month observation. *Psychiatr. Danub.* **23(Suppl. 1)**, S18–S22.
51. Moon, J., Jung, K.H., Shin, J.W., Lim, J.A., Byun, J.I., Lee, S.T., Chu, K. and Lee, S.K. (2014) *Epilepsy Behav.*, **34**, 116–119.
52. Chu, C.C., Wang, J.J., Chen, K.T., Shieh, J.P., Wang, L.K., Shui, H.A. and Ho S.T. (2010) Neurotrophic effects of tianeptine on hippocampal neurons: a proteomic approach. *J. Proteome Res.*, **9**, 936–944.
53. Yamashima, T. (2004) Ca2+-dependent proteases in ischemic neuronal death: a conserved calpain-cathepsin cascade from nematodes to primates. *Cell Calcium*, **36**, 285–293.
54. Pozzo-Miller, L., Pati, S. and Percy, A.K. (2015) Rett syndrome: reaching for clinical trials. *Neurotherapeutics*, **12**, 631–640.
55. Nawaz, M.S., Giarda, E., Bedogni, F., La Montanara, P., Ricciardi, S., Ciceri, D., Alberio, T., Landsberger, N., Rusconi, L. and Kilstrup-Nielsen, C. (2016) CDKL5 and shootin1 interact and concur in regulating neuronal polarization. *PLoS One*, **11**, e0148634.